Journal of Advanced Marine Engineering and Technology, Vol. 45, No. 3, pp. 94~99, 2021
J. Advanced Marine Engineering and Technology (JAMET)
https://doi.org/10.5916/jamet.2021.45.3.94

ISSN 2234-7925 (Print)
ISSN 2765-4796 (Online)
Original Paper

Heat transfer optimization in a vertical cylinder tube with vertically arranged fins

Eunpil Kim†

(Received April 7, 2021 ; Revised May 11, 2021 ; Accepted June 8, 2021)

Abstract: The optimal geometric configuration of a passive heat exchanger in a vertical cylinder is presented herein. The heat exchanger is positioned vertically at the center of the cylinder. Several parameters and flow conditions are investigated to determine the optimized geometric parameters. The finite volume numerical technique is used to obtain computational results. The results show that the number of fins and the cylinder height impose a more significant effect as the inlet velocity increases, whereas the fin height shows similar effects for all inlet velocities tested (1 to 5 m/s). The best heat flux performance is observed at a fin height of 10 mm and a fin count of 58 at a high inlet velocity. A cylinder length of 200 mm is selected considering geometry restrictions.

Keywords: Finite volume scheme, Forced convection, Heat sink, Channel flow

Nomenclature

c_p	specific heat at constant pressure, $J \cdot kg^{-1} \cdot K^{-1}$
d_{in}	inner diameter of cylinder, mm
d_{out}	outer diameter of cylinder, mm
k	thermal conductivity of fluid, $K \cdot m^{-1} \cdot K^{-1}$
h	height of fin, *mm*
L	total length of cylinder, mm
Nu	average Nusselt number
p	pressure, $N \cdot m^{-2}$
T	fluid temperature, K
V	velocity
x_i	coordinate components, *mm*
v_i	velocity components, $m \cdot s^{-1}$

Greek Symbols

ε	turbulent dissipation rate, $m^2 \cdot s^{-3}$
ρ	density
μ_t	viscous dissipation, $m^2 \cdot s^{-3}$
ν	dynamic viscosity, $kg \cdot s^{-1} \cdot m^{-1}$

Subscripts

∞	ambient
in	inlet
out	outlet

1. Introduction

A plate-fin heat exchanger is a passive cooling system that has no external power to an active system. This type of heat exchanger offers a long lifespan, high reliability, and long suitability because it does not require additional equipment for an active system. Hence, it has been used for several decades.

Wang *et al.* **[1]** investigated plate-fin heat exchangers with plain fins and serrated fins. They performed numerical simulations to determine the heat transfer and fluid flow characteristics of heat exchangers with two fins. Grupta *et al.* **[2]** investigated a plate-fin heat exchanger with triangular fins. They demonstrated the flow structure and thermal performance of a winglet vortex generator for heat transfer enhancement. Zhu and Li **[3]** investigated flow and heat transfer characteristics by considering the effects of fin thickness and thermal effects on four types of fins. They presented the results for modified and conventional fin types. In addition, they provided the flow and thermal distribution of a plate-fin heat exchanger. Peng *et al.* **[4]** investigated fin geometry configurations as design parameters and integrated the

† Corresponding Author (ORCID: http://orcid.org/0000-0002-1679-7961): Professor, Department of Refrigeration and Air-Conditioning Engineering, Pukyong National University, 375, Sinseon-ro, Nam-gu, Busan, 608-739, Korea, E-mail: ekim@pknu.ac.kr, Tel: 051-629-6182

design of a cross-plate-fin heat exchanger to optimize the total heat transfer area. Yousefi *et al.* **[5]** proposed a harmony search algorithm for design optimization to obtain the parameter variables. They suggested general optimization methodologies for a multistream plate-fin heat exchanger with fin selection and pressure drop considerations. In addition, they suggested an optimum design solution. Chen and Hsu **[6]** and Chen *et al.* **[7]** used the inverse, finite difference, and least-squares methods for their numerical simulation. In addition, they presented experimental data for predicting the fin efficiency and average heat transfer coefficient of a plate fin and tube heat exchanger with a single tube.

In this study, a plate-fin heat exchanger with a vertically arranged configuration was investigated. The system is used to cool air that is induced in hot ambient environments for a portable cooling system. Forced air flows from the top to the bottom of the system. The optimum geometry configuration of a plate-fin heat exchanger for achieving high heat dissipation performance was determined. Hence, several geometric configurations and flow conditions were investigated.

2. Mathematical Modeling

To obtain the optimized design parameters for a specified geometry, a three-dimensional numerical simulation was performed. A plate-fin heat exchanger located inside a vertical tube was modeled, as shown in **Figure 1**. Additionally, a fan was modeled at the top of the system. Therefore, the air flows from the top to the bottom. (**Figure 1a**). A plate-fin heat exchanger was attached to the outer surface of the inner cylinder. Under the assumption of a thin fin, the fins were vertically located along the circumferential direction. The inner cylinder was positioned inside the center of the outer cylinder. The geometric parameters are shown in **Figure 1b**. **Figure 2** shows the computational domain, which is shown from the entire cylinder.

Considerable computational time is required when performing computational calculations for a three-dimensional geometry. As the geometry investigated is symmetrical along the circular direction, only a portion of the entire three-dimensional cylinder was selected for the computational domain. The domain shows only a section of the cooling air section, which is the main area of observation for the heat dissipation system. Both circular end areas of the cutting geometry had a symmetry boundary condition. The corresponding results were observed in this domain. After performing the computation, the results were recalculated considering the entire system.

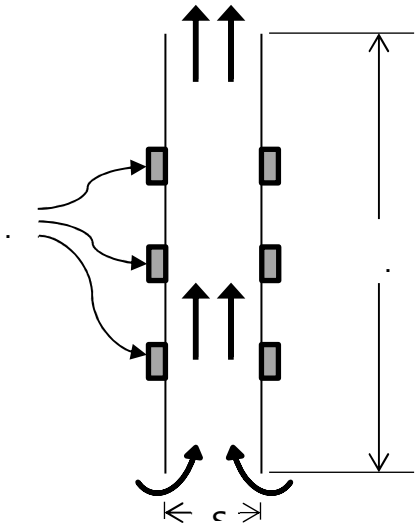

(a) Front view

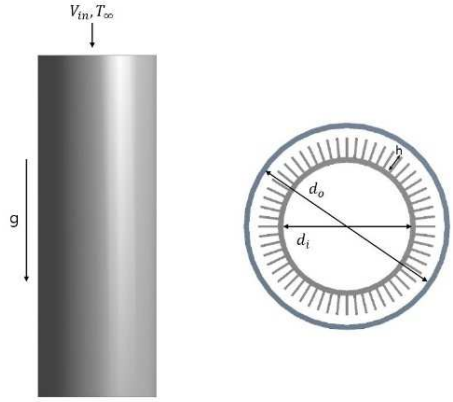

(b) Top view

Figure 1: Schematic illustration of a specified geometry

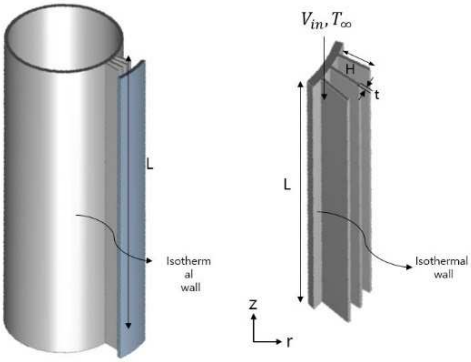

Figure 2: Computational detailed geometry

The initial settings were as follows: The outer diameter of the outer cylinder was 120 mm, and the inner diameter of the inner pipe was 60 mm. The length and thickness of the fin was 10 and 1 mm, respectively. The vertical length of the cylinder was 200 mm. The attached fin count was 50 at the starting point.

The system was simulated under steady-state three-dimensional conditions in forced convection. Hence, the corresponding governing equations of continuity, momentum, and energy were used. The physical properties were assumed to be constant for all situations, including density. The *k–ε* model was used to incorporate turbulence effects. The governing equations are as follows **[2]:**

Continuity:

$$\frac{\partial}{\partial x_i}(\rho u_i) = 0 \tag{1}$$

Momentum:

$$\frac{\partial}{\partial x_j}(\rho u_i u_j) = -\frac{\partial p}{\partial x_i} + \frac{\partial}{\partial x_j}\left[\mu\left(\frac{\partial u_i}{\partial x_j} + \frac{\partial u_j}{\partial x_i} - \frac{2}{3}\delta_{ij}\frac{\partial u_i}{\partial x_j}\right)\right] + \frac{\partial}{\partial x_j}\left(-\rho\overline{u_i' u_j'}\right) \tag{2}$$

Energy:

$$\rho c_p u_i \frac{\partial T}{\partial x_i} = k_c \frac{\partial^2 T}{\partial x_i^2} \tag{3}$$

where ρh is the density, $\mu e$is dynamic viscosity, p the pressure, k_c the thermal conductivity, T the temperature, and α the thermal diffusivity; *u, v, and w* are the velocities in the *x*-, *y*-, and *z*-directions, respectively.

The Reynolds stress, $-\rho\overline{u_i' u_j'}$ must be modeled to complete the equation. For turbulence modeling, the standard *khe* model is typically used. The turbulence-related governing equations are as follows:

The turbulence kinetic energy equation:

$$\frac{\partial}{\partial x_i}(\rho k u_i) = \frac{\partial}{\partial x_j}\left[\left(\mu + \frac{\mu_t}{\sigma_k}\right)\frac{\partial k}{\partial x_j}\right] + \mathrm{G}_k + \mathrm{G}_b - \rho\varepsilon - Y_M + z \tag{4}$$

The turbulence rate of dissipation equation:

$$\frac{\partial}{\partial x_i}(\rho \varepsilon u_i) = \frac{\partial}{\partial x_j}\left[\left(\mu + \frac{\mu_t}{\sigma_\varepsilon}\right)\frac{\partial \varepsilon}{\partial x_j}\right] + C_{1\varepsilon}\frac{\varepsilon}{k}(\mathrm{G}_k + C_{3\varepsilon}\mathrm{G}_b) - C_{2\varepsilon}\rho\frac{\varepsilon^2}{k} + S_\varepsilon \tag{5}$$

where G_k is the generation of turbulent kinetic energy to the mean velocity gradients, and G_b represents the generation of turbulent kinetic energy.

The turbulent viscosity, μ_t, is expressed as follows:

$$\mu_t = \rho C_\mu \frac{k^2}{\varepsilon}, \tag{6}$$

where C_μ is a constant.

The model constants are as follows:

$C_{1\varepsilon} = 1.44;\ C_{2\varepsilon} = 1.92;\ C_\mu = 0.09;\ \sigma_k$=1.0; $\sigma_\varepsilon = 1.3$

To calculate the heat transfer performance, the average Nusselt number with a characteristic length L was evaluated based on the following equation:

$$\overline{Nu} = \frac{\bar{h}L}{k},$$

where $\bar{h}$ is the average heat transfer coefficient, L the cylinder length, and k the thermal conductivity.

The finite control volume method was used to calculate the numerical solution of the governing equations. The second-order upwind method was used for the convective and diffusive terms. The SIMPLER algorithm was used to solve the coupling between the velocity and pressure fields.

Based on an optimized mesh, fluid analysis for various boundary conditions was performed using ANSYS Fluent **[8]**. The mesh was densely distributed near the boundaries, which were positioned at highly variable gradients. Fluid flow can be analyzed by assigning constant inlet boundary conditions and an ambient pressure outlet. The temperature conditions of the cylinders were set as the first boundary condition. Both circular end sections of the cylinder were set as the second boundary condition.

3. Results and discussion

In this section, the computational results of a plate-fin heat exchanger in a forced convection cooling system are presented. The variables of the cooling system were selected to achieve good system performance. As mentioned previously, the parameters of the system were selected by performing numerical simulations. For grid independence, the test was conducted using

various grid numbers (see Kim **[9]**). The geometry parameter and flow condition results are as follows:

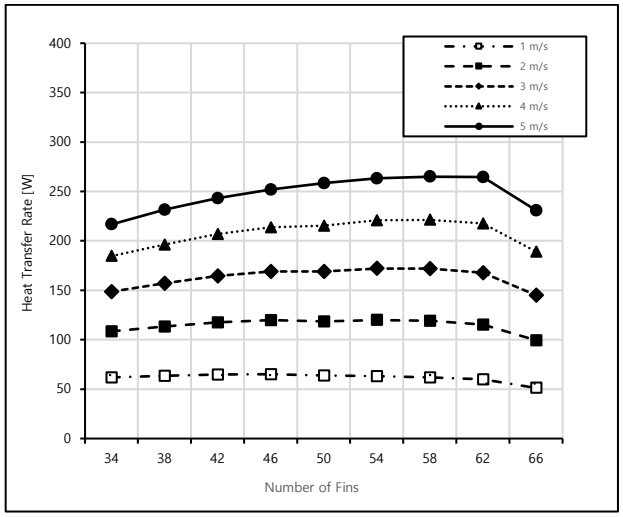

Figure 3: Heat transfer rate variations with different number of fins with inlet velocities

Figure 3 shows the heat transfer rate variation for different fin counts. The inlet velocities were varied from 1 to 5 m/s. For computation, the fin and cylinder heights were set to 10 and 200 mm, respectively, and the fin count was changed from 34 to 66. As shown in **Figure 3**, the heat transfer rates increased with the fin count. This increase continued up to 62 fin counts and then decreased. This is because as the fin count increased, the fin pitch decreased, and the heat transfer area increased. This implies that the flow simultaneously increased the pressure drop and heat transfer. At low inlet velocities, the heat transfer rate was insignificant as the inlet velocities increased. Beyond a 4 m/s inlet velocity, the heat transfer rate increased. Therefore, a fin count of approximately 58 and high inlet velocities provided a favorable heat transfer operation.

Figure 4a shows the temperature contours along the flow direction with the effects of inlet velocities. Cases involving high inlet velocity showed high-temperature transfers from the inlet section. At a high velocity, heat energy is transferred rapidly, as shown clearly in the comparison of temperature difference between the 1 and 5 m/s cases. **Figure 4b** shows the temperature contours at three different locations: the inlet, middle, and outlet sections. These figures are shown in the cutting section at the center of the cylinder. The inlet velocity changed from 1 to 5 m/s, as shown from the left to the right of the figure. The outlet temperature profile shows a clear temperature difference between the extreme cases.

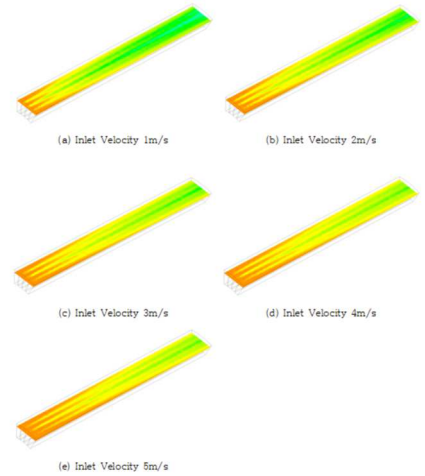

(a)

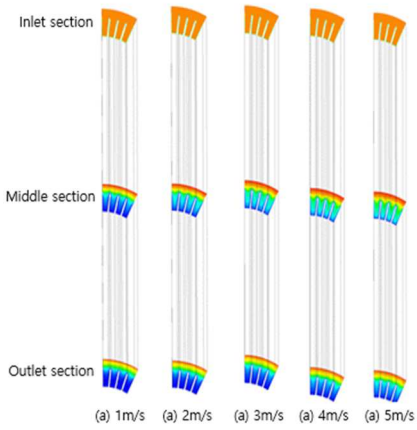

(b)

Figure 4: Temperature contours with different inlet velocities

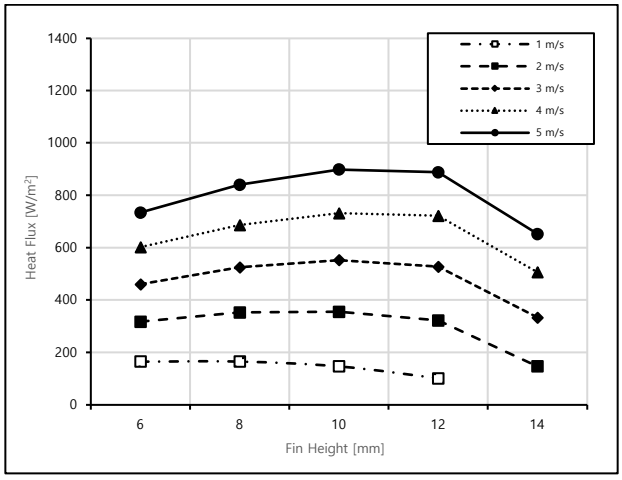

Figure 5: Heat flux variations for different fin heights

Figure 5 shows the heat flux variations for different fin heights. The fins were attached at the inner cylinder surface outwardly. The temperature boundary condition was set to a constant

because of the high thermal conductivity of the fins. As shown in **Figure 5**, the heat flux variations increased with the fin height. When the fin height was 10 mm, the heat flux indicated good performance. Furthermore, the same pattern was exhibited at the high inlet velocities. Beyond 10 mm fin height, the heat transfer did not increase. However, at 14 mm fin height, the heat transfer decreased. Based on **Figure 5**, the best heat flux performance was demonstrated at 10 mm fin height along with high inlet velocities.

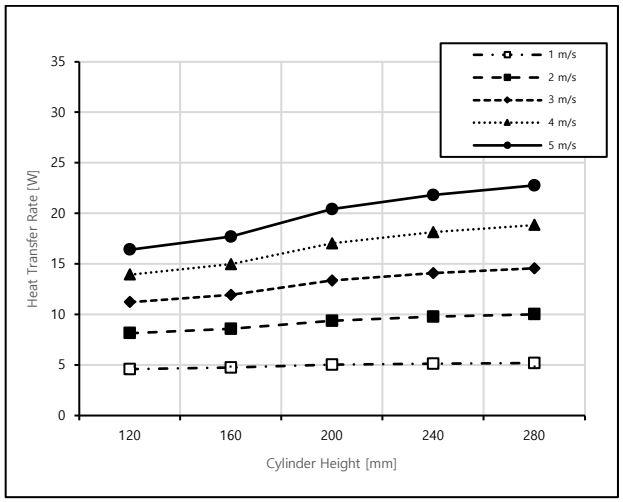

Figure 6: Heat flux variations for different cylinder heights

Figure 6 shows the heat flux variations for different cylinder heights that were positioned vertically. The cylinder height increased from 120 to 200 mm at every 40 mm interval. The cylinder height is a three-dimensional factor that is used to consider the total volume size of the system. As shown in **Figure 6,** the transfer rate increased insignificantly when the inlet velocity was low. However, beyond 3 m/s of inlet velocity, the heat transfer increased significantly compared with the previous increase. At 5 m/s, the heat transfer increased significantly with the increase in the cylinder height. As the cylinder height increased, the heat transfer area increased. A cylinder length of 200 mm was selected, considering the geometry restriction.

Figure 7 shows the temperature distribution of air based on the temperature change of the inner wall. The inner wall corresponded to the fin inside the cooler, and the temperature of the fin changed from 273 to 288 K. The external temperature was set to 303 K. The remaining geometry conditions were set as follows: length of fins, 10 mm; length of cylinder, 200 mm. The cooling boundary effects are clearly shown between the far-right and far-left figures.

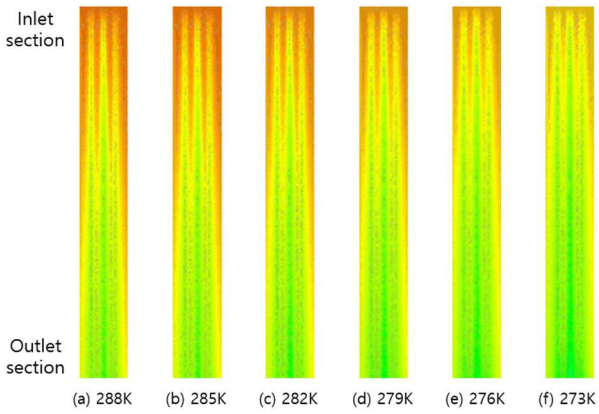

Figure 7: Temperature contours for different inner wall temperatures

Table 1: Net heat flux with different inner wall temperature

	a	b	c	d	e	f
Inwall Temperature [K]	288	285	282	279	276	273
Net Heat Transfer [W]	7.140	9.107	11.069	13.024	14.951	17.041

Table 1 shows the net heat transfer rate when the temperature of the inner wall changed from 273 to 288 K. As shown in **Table 1**, the heat flux decreased as the temperature of the inner wall increased. When the temperature changed by 10°, the heat flow decreased by one-half. Therefore, to improve the thermal dissipation performance, the temperature of the inner wall surface must remain as low as possible.

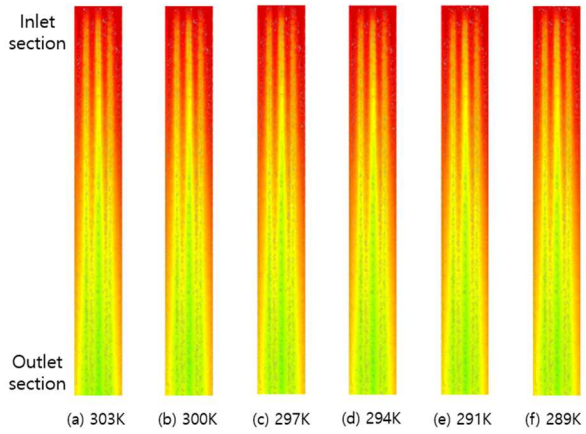

Figure 8: Temperature contours for different outer wall temperatures

Figure 8 shows the temperature distribution of air with temperature changes on the external wall. The external temperature changed from 303 to 289 K. The temperature of the inner fins of

the inner cylinder was set to 273 K. The remaining conditions were set as follows: number of fins, 50; length of fins, 10 mm; length of cylinder, 200 mm. **Figure 8** shows the temperature difference contours between the two extreme cases.

Table 2: Net heat flux with different outer wall temperatures

	a	b	c	d	e	f
Outwall Temperature [K]	303	300	297	294	291	289
Net Heat Transfer [W]	19.711	17.774	15.797	13.823	11.85	10.534

Table 2 shows the net heat transfer rate when the temperature of the outer wall changed from 303 to 289 K. As shown in **Table 2**, the total heat flux decreased as the temperature of the exterior wall decreased linearly.

4. Conclusions

In this study, a plate-fin heat exchanger in a cooling system was investigated. A three-dimensional cylinder-type heat sink with vertical plates was successfully analyzed using the finite volume method. To obtain the optimal configurations, several parameters in a confined geometry were investigated.

At low inlet velocities, the heat transfer effect of the fin count was insignificant. However, a high inlet velocity of approximately 58 fins yielded favorable heat transfer. The best heat flux performance was indicated at a fin height of 10 mm along with high inlet velocities. At 5 m/s, the heat transfer increased significantly with the cylinder height. As the cylinder height increased, the heat transfer area increased. A cylinder length of 200 mm was selected considering the geometry restriction.

Acknowledgement

This work was supported by a Research Grant of Pukyong National University (2019 year)

Author Contributions

Conceptualization, E. Kim; Methodology, E. Kim; Software, E. Kim; Formal Analysis, E. Kim; Investigation, E. Kim; Resources, E. Kim; Data Curation E. Kim; Writing-Original Draft Preparation, E. Kim; Writing-Review & Editing, E. Kim; Visualization, E. Kim; Supervision, E. Kim; Project Administration, E. Kim; Funding Acquisition, E. Kim.

References

[1] Y. Q. Wang, Q. W. Dong, M. S. Liu, and D. Wang, “Numerical study on plate-fin heat exchangers with plain fins and serrated fins at low Reynolds number,” Chemical Engineering Technology, vol. 32, no. 8, pp. 1219-1226, 2009.

[2] M. Gupta, K. S. Kasana, and R. Vasudevan, “A numerical study of the effect on flow structure and heat transfer of a rectangular winglet pair in a plate fin heat exchanger,” Journal of Mechanical Engineering Science, vol. 223, no. 9, pp. 2109-2215, 2009.

[3] Y. Zhu and Y. Li, “Three-dimensional numerical simulation on the Laminar flow and heat transfer in four basic fins of plate-fin heat exchangers,” Journal of Heat Transfer, vol. 130, no. 11, 2008.

[4] H. Peng and X. Ling, “Optimal design approach for the plate-fin heat exchangers using neural networks cooperated with genetic algorithms,” Applied Thermal Engineering, vol. 28, no. 5-6, pp. 642-650, 2008.

[5] M. Yousefi, R. Enayatifar, A. N. Darus, and A. H. Abdullah, “Optimization of plate-fin heat exchangers by an improved harmony search algorithm,” Applied Thermal Engineering, vol. 50, no. 1, pp. 877-885, 2013.

[6] H. T. Chen and W. L. Hsu, “Estimation of heat transfer coefficient on the fin of annular-finned tube heat exchangers in natural convection for various fin spacings,” International Journal of Heat Mass Transfer, vol. 50, no. 9-10, pp. 1750-1761, 2007.

[7] H. T. Chen, Y. S. Lin, P. C. Chen, and J. R. Chang, “Numerical and experimental study of natural convection heat transfer characteristics for vertical plate fin and tube heat exchangers with various tube diameters,” International Journal of Heat Mass Transfer, vol. 100, pp. 320-331, 2016.

[8] ANSYS Inc. Ver. 16, www.ansys.com, Accessed November 21, 2020.

[9] E. P. Kim, “Numerical analysis of a channel flow with two tubes in a vertical plain-fin type heat exchanger,” Journal of the Korean Society Marine Engineering, vol. 41, no. 5, pp. 383-388, 2017.